Preprints of the 21st IFAC World Congress (Virtual)
Berlin, Germany, July 12-17, 2020

Spatial Heterogeneity in Bacterial Cells ⋆

Carlos Barajas * **Domitilla Del Vecchio** *

* *Department of Mechanical Engineering, MIT, Cambridge, MA 02139, USA,(e-mail: carlobar@mit.edu, ddv@mit.edu)*

Abstract:
Commonly used models of genetic circuits assume a well-mixed ensemble of species. However, experimental data suggests that appreciable spatial heterogeneity exists in bacteria cells. There exists no unified modeling framework to capture this spatial phenomena. To this end, we model spatial heterogeneity inside bacterial cells and propose a simple framework that accounts for spatial information. In this document, we start with a generic spatial-temporal partial differential equitation (PDE) model. Then, we exploit time scale separation between diffusion and the reaction dynamics to derive a reduced model consisting solely of ordinary differential equations (ODEs). This result is then applied to study an enzymatic-like reaction. It is shown that spatial heterogeneity modifies the binding strength between two species that reversibly bind to each other. We show that the modified binding rate for certain cases can be larger or smaller than that of a well-mixed model. Therefore, this work takes a step forward towards creating a general and simple framework to model spatial heterogeneity in bacterial cells and thus improving the predictive power of current models that are used to design genetic circuits

Keywords: genetic circuits, model reduction, biomolecular systems, reaction-diffusion

1. INTRODUCTION

Deterministic models of gene networks typically assume a well-mixed ensemble of species inside the cell (Del Vecchio and Murray (2017)). However, it is well known that spatial heterogeneity is prevalent inside the cell (Wingreen and Huang (2015); Weng and Xiao (2014)). Depending on the origin of replication, plasmids tend to localize within bacterial cells (Wang et al. (2016)). Furthermore, chromosome genes are distributed in the cell according to the chromosomes complex spatial structure. In bacterial cells, any species freely diffusing through the chromosome (e.g., mRNA, ribosome, and protease) experiences what are known as *excluded volume effects*, which is the tendency for the species to be ejected from the nucleoid due to the space occupied by the dense DNA mesh (Castellana et al. (2016)). These excluded volume effects for ribosomes and RNAP in bacteria have been observed experimentally (Bakshi et al. (2012)).

Despite the strong evidence against a well-mixed model, no standard modeling framework exists for genetic circuits that captures the spatial-temporal organization inside the cell. Furthermore, current approaches that rely solely on numerical simulations of partial differential equations (PDEs) may be impractical for genetic circuit design.

In this abstract, we present a model reduction strategy starting from a system of coupled PDEs and ODEs to a reduced system of ODEs via timescale separation between diffusion and the reaction dynamics. By applying this result to an enzymatic-like reaction, we demonstrate that the reduced model accounts for spatial heterogeneity in the spaced averaged dynamics by multiplying the association rate constant of bimolecular interactions by a correction factor that depends on spatial information. Thus, this reduced model has similar computational cost as current well-mixed models, yet it captures spatial effects. Specifically, we focus on capturing excluded volume effects and gene location information. We analyze the correction factor in two different cases: when the enzyme and substrate both diffuse (mRNA-sRNA, protein-protease- mRNA-ribosomes) and when the enzyme diffuses and the substrate is fixed in space (transcription factor-DNA,protein-membrane). This analysis provides insight into how effectively species interact depending on their size and the location where they are fixed.

2. RESULTS

Notation: Let $\boldsymbol{z} = [z_1, \ldots, z_n]^T \in \mathbb{R}^n$ (where superscript T denotes the transpose operation) and the j-th component of $\boldsymbol{z}$ is denoted by $\boldsymbol{z}^j$. A vector of zeros is denoted as $\boldsymbol{0}_n = [0, \ldots, 0]^T \in \mathbb{R}^n$ and we use $\boldsymbol{A} = \text{diag}(\boldsymbol{u}) \in \mathbb{R}^{n \times n}$ to refer to a square matrix with all zeros in the off-diagonals and diagonal elements specified by the vector $\boldsymbol{u} \in \mathbb{R}^n$. $\mathbb{R}^n_+$ denotes the positive orthant of $\mathbb{R}^n$. Let $\Omega = (0, 1)$, $\overline{\Omega} = [0, 1]$, $\partial\Omega = \{0, 1\}$.

The model used to capture intracellular species interacting as they diffuse inside the cell is now introduced. As in Castellana et al. (2016), we assume the cell to have a cylindrical geometry, angular symmetry, and radial homogeneity such that the concentration of a species varies only axially (the spatial x direction). Symmetry relative to the mid-cell is assumed and hence only half of the cell is considered; $x \in [0, 1]$, where $x = 0$ is at the mid-cell and $x = 1$ is at the cell poles. Furthermore, we assume a constant cross-sectional area along the axial

⋆ This work was supported by NSF award number 1521925

direction. Let $\boldsymbol{v} : \bar{\Omega} \to \mathbb{R}_+^{n_d}$ be a smooth vector-valued function and $\boldsymbol{V}(x) = \text{diag}(\boldsymbol{v}(x))$. For the state vectors $\boldsymbol{z}_s(t,x) \in L^2(\Omega, \mathbb{R}^{n_s})$ and $\boldsymbol{z}_d(t,x) \in L^2(\Omega, \mathbb{R}^{n_d})$, consider the following reaction diffusion system:

$$\frac{\partial \boldsymbol{z}_s(t,x)}{\partial t} = \boldsymbol{f}_s(t,x,\boldsymbol{z}_s,\boldsymbol{z}_d), \quad t>0, x \in \bar{\Omega}, \tag{1a}$$

$$\frac{\partial \boldsymbol{z}_d(t,x)}{\partial t} = \frac{1}{\epsilon}\boldsymbol{\mathcal{L}}(\boldsymbol{z}_d) + \boldsymbol{f}_d(t,x,\boldsymbol{z}_s,\boldsymbol{z}_d), \quad t>0, x \in \Omega, \tag{1b}$$

$$\boldsymbol{V}(x)\frac{d}{dx}\big[\boldsymbol{V}^{-1}(x)\boldsymbol{z}_d(t,x)\big] = \boldsymbol{0}_n \quad t>0, x \in \partial\Omega \tag{1c}$$

$$\boldsymbol{z}_s(0,x) = \boldsymbol{z}_{s,0}(x), \quad x \in \Omega, \tag{1d}$$

$$\boldsymbol{z}_d(0,x) = \boldsymbol{z}_{d,0}(x), \quad x \in \Omega, \tag{1e}$$

$$\boldsymbol{\mathcal{L}}^i(\boldsymbol{z}_d) = D_i \frac{d}{dx}\left[(\boldsymbol{v}^i(x))^2 \frac{d}{dx}\left[\frac{\boldsymbol{z}_d^i(t,x)}{\boldsymbol{v}^i(x)}\right]\right], \tag{1f}$$

$D_i \in \mathbb{R}_+$, $\epsilon \in \mathbb{R}_+$, $\boldsymbol{f}_s : [0,\infty) \times \bar{\Omega} \times \mathbb{R}^{n_s} \times \mathbb{R}^{n_d} \to \mathbb{R}^{n_s}$ and $\boldsymbol{f}_d : [0,\infty) \times \bar{\Omega} \times \mathbb{R}^{n_s} \times \mathbb{R}^{n_d} \to \mathbb{R}^{n_d}$ are smooth nonlinear functions, $\boldsymbol{z}_{s,0}^i : \bar{\Omega} \to \mathbb{R}+$, and $\boldsymbol{z}_{d,0}^i : \bar{\Omega} \to \mathbb{R}_+$. In (1), $\boldsymbol{z}_s$ corresponds to spatial fixed species (e.g., DNA) and $\boldsymbol{z}_d$ to diffusing species (e.g., Ribosomes).

The expression for the flux dynamics (1f) was derived in (Castellana et al. (2016)) and captures excluded volume effects via $\boldsymbol{v}^i(x)$, which is the fraction of volume available for a species to diffuse within the chromosome mesh. DNA localization can be modeled explicitly in $\boldsymbol{f}_s$.

Next, we define the candidate reduced order model that will serve as an approximation to (1) in the limit of fast diffusion ($\epsilon \to 0^+$).

Definition 1. (Reduced slow dynamics) Let the state vectors $\hat{\boldsymbol{z}}_s(t,x) \in \mathbb{R}^{n_s}$ and $\hat{\boldsymbol{z}}_d(t,x) \in \mathbb{R}^{n_d}$ satisfy

$$\frac{\partial \hat{\boldsymbol{z}}_s(t,x)}{\partial t} = \boldsymbol{f}_s(t,x,\hat{\boldsymbol{z}}_s,\hat{\boldsymbol{z}}_d), \quad t>0, x \in \bar{\Omega}, \tag{2a}$$

$$\frac{\partial \hat{\boldsymbol{z}}_d(t,x)}{\partial t} = \hat{\boldsymbol{V}}(x)\int_\Omega \boldsymbol{f}_d(t,x,\hat{\boldsymbol{z}}_s,\hat{\boldsymbol{z}}_d), \quad t>0, x \in \bar{\Omega}, \tag{2b}$$

$$\hat{\boldsymbol{z}}_s(0,x) = \boldsymbol{z}_{s,0}(x), \quad x \in \Omega, \tag{2c}$$

$$\hat{\boldsymbol{z}}_d(0,x) = \hat{\boldsymbol{V}}(x)\int_\Omega \boldsymbol{z}_{d,0}(x). \tag{2d}$$

where $\hat{\boldsymbol{V}}(x) = \frac{\boldsymbol{V}(x)}{\int_\Omega \boldsymbol{V}(x)}$. From (2), the dynamics for the fixed species are the same as (1a) , but for the diffusing species, they take place in the null space of (1f) (span of $\boldsymbol{v}^i(x)$) and thus

$$\hat{\boldsymbol{z}}_d(t,x) = \hat{V}(x)\hat{\bar{\boldsymbol{z}}}_{\boldsymbol{d}}(t) \tag{3}$$

where $\hat{\bar{\boldsymbol{z}}}_{\boldsymbol{d}}(t) = \int_\Omega \hat{\boldsymbol{z}}_d(t,x)$. From (3) we see that $\hat{\boldsymbol{z}}_d(t,x)$ mirrors $\hat{V}(x)$ spatially.

The following result holds if the vector field $[\boldsymbol{f}_s, \boldsymbol{f}_d]$ points inwards at the boundaries of a closed convex subset of $\mathbb{R}^{n_d+n_s}$, which implies the set is positively invariant (Weinberger (1975)), and if the reduced dynamics are robust to an $\mathcal{O}(\epsilon)$ disturbance. That is, solutions remain $\mathcal{O}(\epsilon)$ close when an $\mathcal{O}(\epsilon)$ disturbance is present in the dynamics. *Main Result:* Let $\boldsymbol{z}_s$ and $\boldsymbol{z}_d$ be given by (1) and $\hat{\boldsymbol{z}}_s$ and $\hat{\boldsymbol{z}}_d$ be given by (2), in our work we show that as $\epsilon \to 0^+$, there exists $\delta > 0$ such that for all $t \geq 0$:

$$\boldsymbol{z}_s(t,x) = \hat{\boldsymbol{z}}_s(t,x) + \mathcal{O}(e^{-\frac{\delta}{\epsilon}t}) + \mathcal{O}(\epsilon),$$
$$\boldsymbol{z}_d(t,x) = \hat{\boldsymbol{z}}_d(t,x) + \mathcal{O}(e^{-\frac{\delta}{\epsilon}t}) + \mathcal{O}(\epsilon).$$

3. APPLICATIONS

We consider an enzymatic-like reaction to apply our result and highlight the role of spatial heterogeneity on bimolecular dynamics. We model substrate S binding to enzyme E to form product P. To account for spatial heterogeneity, using the results in the previous section, one can consider a standard ODE model derived from mass action kinetics (Del Vecchio and Murray (2017)) corresponding to the biochemical reactions given by:

$$\text{E} + \text{S} \underset{\text{d}}{\overset{\text{a}\theta}{\rightleftharpoons}} \text{c} \xrightarrow{\kappa} \text{P} + \text{E} + \text{S}, \tag{4}$$

where c is the complex formed when E binds to S, a is the association rate constant, d is the dissociation rate constant, and κ is the catalytic rate of formation. Spatial information is captured via parameter θ and it is approximated using our theoretical results by θ^*. For a well-mixed model $\theta = 1$. We determine θ^* for:

Case I: E and S both freely diffuse (e.g., mRNA (E) being translated by ribosome (S))

Case II: E freely diffuses and S is spatially fixed at $x = x^*$ (e.g., RNAP (E) transcribing DNA (S))

For Case II, S spatially fixed at $x = x^*$ corresponds to its production rate confined to a small region around x^*. A graphical representation of θ^* for Cases I-II is shown in Figure 1 as species size and localization point x^* vary.

For Case I, when E (size r_e) and S (size r_s) are sufficiently large, then $\theta^* > 1$ and thus always greater than that of the well-mixed model ($\theta^* = 1$) and this discrepancy increases with their size. The upper bound for θ^* is $1/\Delta x$ (where Δx is the distance between the end of the chromosome and the cell poles). Notice that if $r_e/r^* \gg 1$ and $r_s/r^* \ll 1$ (or vice versa), then $\theta^* \approx 1$ and thus a well-mixed model is appropriate despite severe intracellular heterogeneity.

For Case II, when $r_e/r^* \ll 1$, then $\theta^* \approx 1$. When $r_e/r^* \gg 1$, then $\theta^* < 1$ (even zero) when the fixed species is localized near mid-cell ($x^* \approx 0$) and $\theta^* < 1$ (upper bounded by θ^* is $1/\Delta x$) when the fixed species is localized near the cell-poles ($x^* \approx 1$). There is a region near quarter-cell ($x \approx 0.5$) where $\theta^* \approx 1$ for all values of r_e.

When (4) corresponds to an mRNA (E) binding to a ribosome (S)(Case I), we can conclude that the rate of translation predicted by a model that includes spatial heterogeneity is higher than that of a well-mixed model. This is because both the mRNA and the ribosome are excluded out of the chromosome onto the cell poles and thus are more likely to bind in this confined region.

When (4) corresponds to RNAP (E) binding to a DNA (S) (Case II), we conclude that the rate of transcription predicted by a model that includes spatial heterogeneity depends on the location of the DNA. If the DNA is in the cell-poles (mid-cell), then transcription higher (lower) than that of a well-mixed model. Intuitively, as RNAP is ejected from the chromosome via excluded volume effects, it is more likely to bind to pole localized genes than those near the dense chromosome.

4. CONCLUSION

In this extended abstract we performed model reduction of a general diffusion-reaction system that includes freely dif-

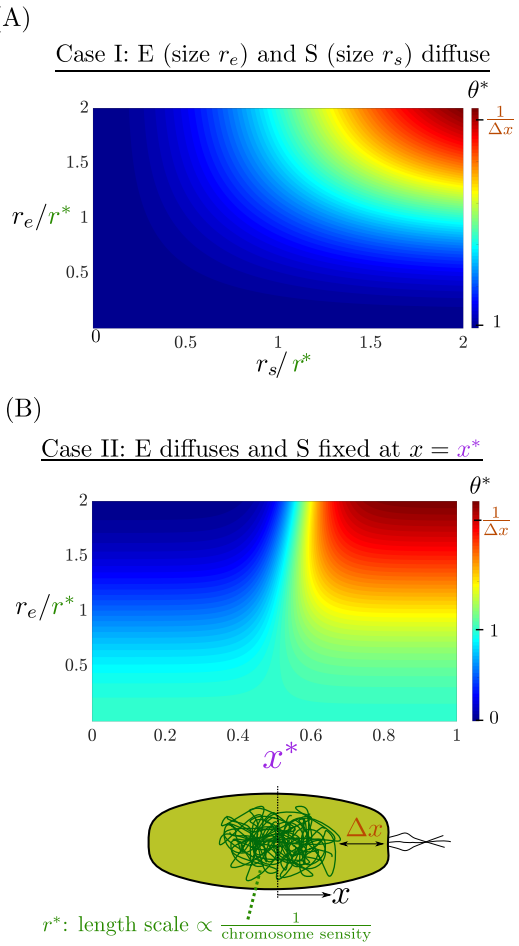

Fig. 1. θ^* **as species size and localization varies**. (A) Case I: $\theta^* \geq 1$ and increases with the size of E and S (upper bounded by $1/\Delta x$). If E or S is sufficiently small, then $\theta^* \approx 1$. (B) Case II: For sufficiently small E, then $\theta^* \approx 1$. When E is sufficiently large, then if $x^* \approx 0$, it implies that $\theta^* < 1$ (may even be zero) and if $x^* \approx 1$, it implies that $\theta^* > 1$ (upper bounded by $1/\Delta x$). Here, Δx is the distance between the end of the chromosome and the cell poles.

fusing and stationary species within the cell via time scale separation between the diffusion and reaction dynamics. The reduced model consists of a set of pointwise ODEs with no spatial differential terms. By applying our result to an enzymatic-like reaction, we showed that the space averaged dynamics corresponding to the reduced model incorporates spatial heterogeneity by modifying the association rate constant between the enzyme and the substrate. In the case where both the enzyme and substrate diffuse freely, the effective binding is greater than that of a well-mixed model and increased with the size of both species. In the case where the enzyme freely diffused but the substrate is fixed at some spatial location, then the effective binding is greater (smaller) than that of a well-mixed model when the substrate is localized near the cell poles (mid-cell) and this discrepancy increased with the size of the enzyme. We also showed that a well-mixed model may be appropriate despite severe intracellular heterogeneity.

The reactions in (4) can easily be extended to the case where n enzymes compete for a common substrate. The interaction between each enzyme and the substrate will get their own modification factor. This could be used to model n mRNA competing for ribosomes or n transcription factors binding to a single gene. We applied our results of Case I, to model freely diffusing mRNA's being translated by freely diffusing ribosomes, but we can easily consider co-transcriptional translation (this falls under Case II).

In future work we will address the case when part of the reaction dynamics are of the same timescale as diffusion (e.g., fast binding and unbinding). Preliminary work suggest that all results provided here apply in the case of fast binding and unbinding. Future models should capture crowding (Tabaka et al. (2014)), although (1f) accounts for crowding (via the diffusion coefficient, see Castellana et al. (2016)), but it may be modeled more explicitly in the diffusion operator. Finally, we only assumed spatial heterogeneity in a single dimension (axially), but in future work to capture more spatially complex processes in the cell (e.g., processes that occur near the cell membrane), we would like to account spatial variations in the radial and angular directions.

REFERENCES

Bakshi, S., Siryaporn, A., Goulian, M., and Weisshaar, J.C. (2012). Superresolution imaging of ribosomes and RNA polymerase in live Escherichia coli cells. *Mol. Microbiol.*, 85(1), 21–38. doi:10.1111/j.1365-2958.2012.08081.x.

Castellana, M., Hsin-Jung Li, S., and Wingreen, N.S. (2016). Spatial organization of bacterial transcription and translation. *Proc. Natl. Acad. Sci.*, 113(33), 9286–9291. doi:10.1073/pnas.1604995113.

Del Vecchio, D. and Murray, R.M. (2017). *Biomolecular Feedback Systems*. doi:10.23943/princeton/9780691161532.001.0001.

Soh, S., Byrska, M., Kandere-Grzybowska, K., and Grzybowski, B.A. (2010). Reaction-diffusion systems in intracellular molecular transport and control. *Angew. Chemie - Int. Ed.*, 49(25), 4170–4198. doi:10.1002/anie.200905513.

Tabaka, M., Kalwarczyk, T., Szymanski, J., Hou, S., and Holyst, R. (2014). The effect of macromolecular crowding on mobility of biomolecules, association kinetics, and gene expression in living cells. *Front. Phys.*, 2(September), 1–14. doi:10.3389/fphy.2014.00054.

Wang, Y., Penkul, P., and Milstein, J.N. (2016). Quantitative Localization Microscopy Reveals a Novel Organization of a High-Copy Number Plasmid. *Biophys. J.*, 111(3), 467–479. doi:10.1016/j.bpj.2016.06.033. URL `http://dx.doi.org/10.1016/j.bpj.2016.06.033`.

Weinberger, H. (1975). Invariant sets for weakly coupled parabolic and elliptic systems. *Rend. Mat. Univ. Roma*, 8(1), 295–310.

Weng, X. and Xiao, J. (2014). Spatial organization of transcription in bacterial cells. *Trends Genet.*, 30(7), 287–297. doi:10.1016/j.tig.2014.04.008. URL `http://dx.doi.org/10.1016/j.tig.2014.04.008`.

Wingreen, N.S. and Huang, K.C. (2015). Physics of Intracellular Organization in Bacteria. *Annu. Rev. Microbiol.*, 69(1), 361–379. doi:10.1146/annurev-micro-091014-104313.